Proc. Indian Acad. Sci. (Chem. Sci.), Vol. 102, No. 3, June 1990, pp. 195–202.

Ferroverdin: Cation variation and recognition of isomeric *tris* chelate geometries by iron oxidation states

SURAJIT CHATTOPADHYAY, PARTHA BASU, DEBASHIS RAY, SAMUDRANIL PAL and ANIMESH CHAKRAVORTY*

Department of Ironganic Chemistry, Indian Association for the Cultivation of Science, Calcutta 700032, India

Abstract. Synthetic ferroverdins, $NaFe^{II}(RQ)_3$ afford trinuclear $M[Fe(RQ)_3]_2$ upon reaction with bivalent ions (M^{2+}). A probable bonding mode is considered. Ferric ions oxidise ferroverdin to ferriverdin, $Fe^{III}(RQ)_3$. Both *fac* and *mer* isomers can be observed for ferro- and ferriverdins but at equilibrium the preferred isomers are *fac* for ferro- and *mer* for ferriverdin. Mismatch in geometry with oxidation state gets spontaneously corrected by isomerisation. Equilibrium constants, isomerisation rates, redox potentials and EPR spectra are examined. A study on the pattern of isomer population as a function of oxidation for other 3*d* analogues of ferro- and ferriverdin is initiated.

Keywords. Ferroverdin; ferriverdin; trinucleation; redox regulated isomerism.

1. Introduction

In the course of a search for antifungal antibiotics, a streptomycete was isolated from soil which produced an intense green pigment on yeast agar. The pigment can be produced in submerged cultures and was shown to be an iron complex which was named 'ferroverdin' (Chain *et al* 1955). In this work we summarise aspects of ferroverdin chemistry dealing with composition and stereodynamic redox behaviour. Detailed reports on some features are already available elsewhere (Ray and Chakravorty 1988; Basu *et al* 1989).

2. Results and discussion

2.1 *Outline of work*

A single crystal X-ray crystallographic study (Candeloro *et al* 1969) of one preparation of ferroverdin demonstrated that the pigment contains the *tris* chelate anion (figure 1) in facial configuration (figure 2); the counter-cation is Na^+ and R is [*p*-$(CH_2{=}CH)C_6H_4OC(=O)$–]. The bivalent iron atom is low-spin (Ehrenberg 1956). Different preparations of ferroverdin however differ in iron content and it has been conjectured that this might be due to counter-cation variation (Candeloro *et al* 1969). We wanted to understand the nature and extent of such variation.

* For correspondence

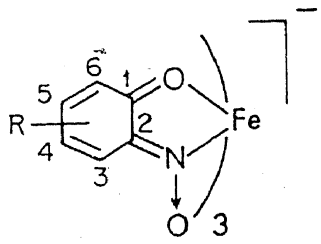

Figure 1. The ferroverdin family (cation not shown).

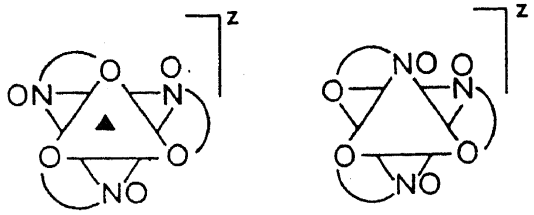

Figure 2. Geometrical isomers of ferroverdin ($z = -1$) and ferriverdin ($z = 0$).

In the course of this scrutiny we were led to react ferroverdin analogues (see below) with Fe^{3+} and Ag^{+} ions. These reagents were found to oxidise the metal centre of the analogues to the trivalent state. This led us to the discovery of a dynamic relationship between metal redox and *tris* chelate geometry.

2.2 *Synthetic ferroverdins*

The natural ferroverdin pigment was not available to us and we employed synthetic members of the same chemical family – the ferroverdin family (figure 1). The general abbreviation for the sodium salts is $NaFe(RQ)_3$ where R represents 4-Me, 4-^{t}Bu, 4-Cl, 4-Br or 3,4-benzo (abbreviated Bz). The green diamagnetic complexes were prepared by *in situ* nitrosation of the corresponding phenols in the presence of iron(II) salts (Baudisch 1940; Cronheim 1947; Charalambous *et al* 1987). The electronic spectra of natural ferroverdin and $NaFe(RQ)_3$ are very similar and have diagnostic bands near 450 nm and 700 nm. The synthetic ferroverdins like the natural one has facial geometry (Basu *et al* 1989a, b).

2.3 *Replacement of Na^{+} with bivalent cations, M^{2+}*

These experiments were performed with $NaFe(MeQ)_3$. In methanol solution this complex reacts smoothly with bivalent ions such as Mg^{2+}, Ca^{2+}, Mn^{2+}, Fe^{2+}, Co^{2+}, Ni^{2+}, Zn^{2+} and Cd^{2+} affording trinuclear $M[Fe(MeQ)_3]_2$.

We have not succeeded so far in growing X-ray quality single crystals of any of the $M[Fe(MeQ)_3]_2$ species and their molecular structure remains uncertain at present. However, on the basis of analogy with arylazooximates (Pal *et al* 1985, 1986; Pal and Chakravorty 1987), a structure as in figure 3 is proposed. In this each facial $Fe(MeQ)_3^-$ moiety acts as a tridentate O_3 (oximato oxygen atoms) ligand and two of these sequester the M^{2+} in the octahedral O_6 sphere.

Upon treating $M[Fe(MeQ)_3]_2$ in acetone solution with aqueous NaOH in the mole ratio 1:2, $M(OH)_2$ gets precipitated quantitatively and $NaFe(MeQ)_3$ is

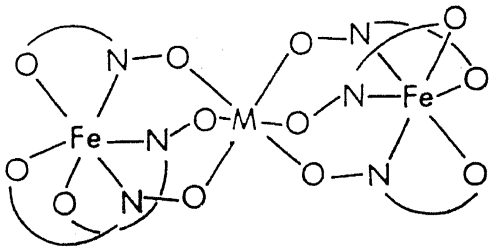

Figure 3. Proposed structure of $M[Fe(RQ)_3]_2$.

regenerated. The aggregation of $M[Fe(MeQ)_3]_2$ from $Fe(MeQ)_3^-$ and M^{2+} and its segregation by alkali finds ready rationalisation in the structure shown in figure 3. During aggregation $Fe(MeQ)_3^-$ sequesters M^{2+} and during segregation OH^- displaces $Fe(MeQ)_3^-$.

The radii of the ions utilised in the present work for trinucleation span the range 0·68 to 1·06 Å. The radii of Sr^{2+} (1·27 Å) and Ba^{2+} (1·43 Å) which fail to afford $M[Fe(MeQ)_3]_2$ are larger. The significance of this is unclear at present but it may be related to the viable size of the octahedral O_6 cavity.

The conjecture that Na^+ in different ferroverdin preparations 'may be replaced by other ions – even perhaps sometimes by additional ferrous ion' is justified (Candeloro *et al* 1969; Basu *et al* 1989c).

2.4 *Oxidation of ferroverdin to ferriverdin*

Success in generating the trinuclear $M^{II}Fe_2N_6O_6$ complexes led us to attempt trinucleation with Fe^{3+} with the hope of obtaining the mixed valence $Fe^{III}Fe^{II}{}_2N_6O_6$ system. This did not succeed. Instead Fe^{3+} quantitatively oxidises green $Fe^{II}(RQ)_3^-$ to brown $Fe^{III}(RQ)_3$. The latter is called ferriverdin. Exactly one mole of Fe^{3+} is required for oxidation of one mole of $Fe(RQ)_3^-$. The same oxidation can be achieved with the help of silver perchlorate.

2.5 *Ferriverdin isomers*

The frozen glass (77 K) EPR spectra (figure 4) of solutions freshly oxidised at 253 K or below are axial, showing that facial $Fe(RQ)_3$ is stereoretentively formed by oxidation of facial $Fe(RQ)_3^-$. When the oxidised solutions are left to equilibriate at 298 K the EPR spectrum becomes rhombic showing that *fac*-$Fe(RQ)_3$ has isomerised to *mer*-$Fe(RQ)_3$. The latter can be isolated in a pure form from the reaction mixture.

Both *fac* and *mer*-$Fe(RQ)_3$ are low-spin ($S = 1/2$) and the EPR data have been analysed with the help of the g-tensor theory of the low-spin d^5 complexes (Bleaney and O'Brien 1956; Griffith 1961; Lahiri *et al* 1987). In this manner the energies ΔE_1 and ΔE_2 of the ligand transitions from the EPR active Kramers doublet to the upper two can be calculated. The ΔE_2 transition has been experimentally observed in the case of *mer*-$Fe(RQ)_3$. The other transitions have inconveniently low energies for observation. EPR g-values as well as ΔE_1 and ΔE_2 values are collected in table 1.

2.6 *Electrochemical mapping of isomerisation equilibria*

The oxidation of *fac*-ferroverdin to *fac*-ferriverdin and the subsequent isomerisation

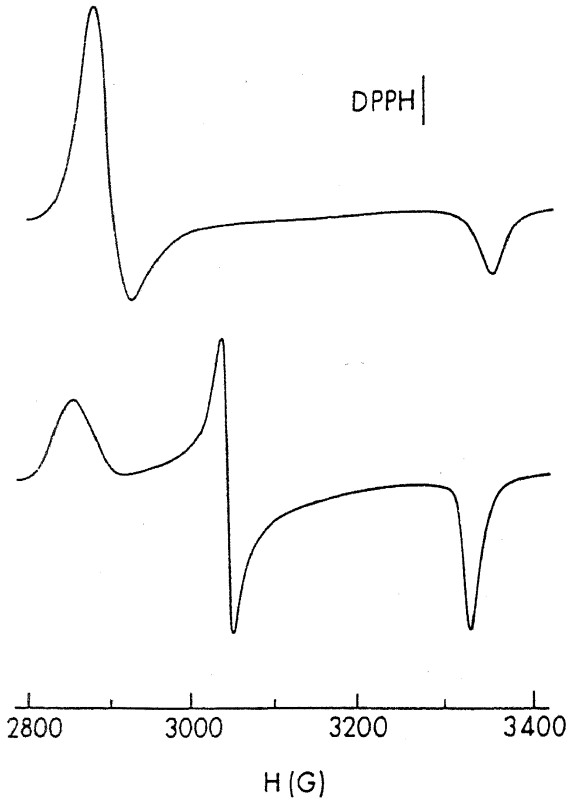

Figure 4. EPR spectra of $Fe(MeQ)_3$ in acetonitrile–toluene glass (77 K): top, initial spectrum (*fac* isomer); bottom, final spectrum (*mer* isomer).

Table 1. EPR *g*-values and near-IR transitions.

Compound	Isomer	*g*-Values	ΔE_1 (cm^{-1})	ΔE_2 (cm^{-1}) Calculated	ΔE_2 (cm^{-1}) Observed
$Fe^{III}(MeQ)_3^*$	*fac*	2·263, 1·959	3560	3940	
	mer	2·294, 2·159, 1·971	3480	6180	5400
$Fe^{III}(ClQ)_3^*$	*fac*	2·259, 1·960	3600	3980	
	mer	2·296, 2·150, 1·970	3350	6270	5500
$Fe^{III}(BzQ)_3^\dagger$	*fac*	2·317, 1·940	2940	3320	
	mer	2·350, 2·224, 1·957	3080	4690	4240

*In acetonitrile–toluene (1:1) glass (77 K); †in dimethylformamide–toluene (1:1) glass (77 K).

of the latter has a counterpart in the reduction of *mer*-ferriverdin into *mer*-ferroverdin which spontaneously isomerises to *fac*-ferroverdin. These changes depicted in figure 5 can be mapped electrochemically. The ferriverdin/ferroverdin reduction potentials are listed in table 2. Representative isomer voltammograms are shown in figure 6. It is believed that the higher ligand field axial distortion of the *mer* isomer is at least partly responsible for the lower value of $E^0(mer)$ compared to $E^0(fac)$, table 2 (Basu *et al* 1989a). Low-spin d^5–d^6 redox couples of *fac* and *mer* isomers are documented among carbonyl complexes. The $E^0(fac) > E^0(mer)$ relation is valid in these cases also (Bond *et al* 1986). Better π-stabilisation of the redox orbital in the reduced (d^6) *fac* isomer is believed to be a reason (Bursten *et al* 1982).

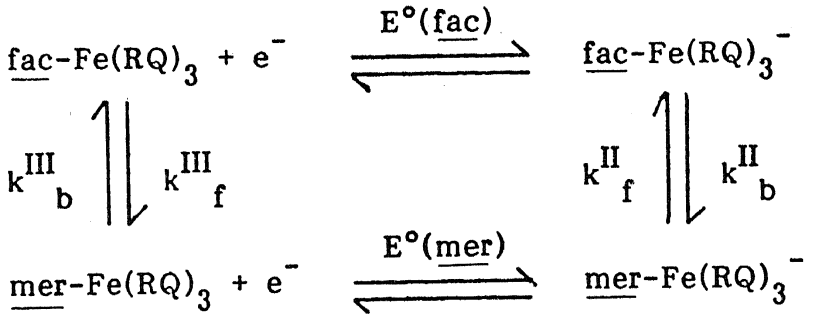

Figure 5. Ferroverdin–ferriverdin *fac–mer* redox–isomerisation cycle.

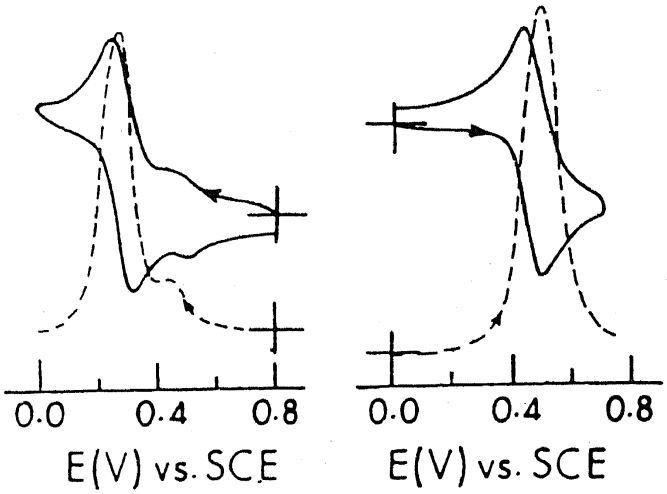

Figure 6. Cyclic and differential pulse voltammograms of equilibrated solutions in MeCN: left, $Fe(MeQ)_3$; right, $Fe(MeQ)_3^-$.

Table 2. Cyclic voltammetric reduction potentials (E^0 in volts) and peak-to-peak separations (ΔE_p in mvolts) at platinum electrode (298 K; supporting electrolyte teap).

R	Solvent	$E^0(fac), \Delta E_p$	$E^0(mer), \Delta E_p$
Me	MeCN	0·45, 60	0·26, 80
'Bu	MeCN	0·48, 60	0·29, 60
Cl	MeCN	0·72, 60	0·53, 60
Br	MeCN	0·75, 60	0·55, 70
Bz	DMF	0·39, 60	0·27, 60

Table 3. Equilibrium constants at 298 K.

R	Solvent	$10^{-3}K^{cr}$	K^{III}	$10^{-2}K^{II}$
Me	MeCN	1·6	6·5	2·5
'Bu	MeCN	1·6	5·7	2·9
Cl	MeCN	1·6	7·9	2·1
Br	MeCN	2·4	8·0	3·0
Bz	DMF	0·11	5·5	0·19

Relevant equilibrium constants are defined below and the results summarised in table 3. These are considered again in a later section.

$$K^{III} = k^{III}{}_f / k^{III}{}_b = [mer\text{-}Fe(RQ)_3]/[fac\text{-}Fe(RQ)_3] \quad (1)$$

$$K^{II} = k^{II}{}_f / k^{II}{}_b = [fac\text{-}Fe(RQ)_3^-]/[mer\text{-}Fe(RQ)_3^-] \quad (2)$$

$$fac\text{-}Fe(RQ)_3 + mer\text{-}Fe(RQ)_3^- \overset{K^{cr}}{\rightleftharpoons} fac\text{-}Fe(RQ)_3^- + mer\text{-}Fe(RQ)_3$$

$$K^{cr} = K^{III}K^{II} = \exp\left[\frac{F}{RT}(E_T^0(fac) - E_T^0(mer)\right] \quad (3)$$

Table 4. Rate constants.

R	Solvent	Temperature (K)	k^{III}_f	k^{II}_f
Me	MeCN	302	$2{\cdot}37 \times 10^{-3}$	$5{\cdot}04 \times 10^{-4}$
^{t}Bu	MeCN	320	$1{\cdot}71 \times 10^{-3}$	—
Cl	MeCN	292	$8{\cdot}58 \times 10^{-3}$	—
		310	—	$1{\cdot}23 \times 10^{-4}$
Bz	DMF	298	$13{\cdot}4 \times 10^{-3}$	$3{\cdot}9 \times 10^{-4}$

2.7 *Rates of isomerisation*

Since K^{III} and K^{II} are known, only two rate constants such as k^{III}_f and k^{II}_f are actually required to be determined for defining the rates in figure 5. Rates were determined spectrophotometrically and selected results are stated in table 4.

Variable temperature rate constants and activation parameters were determined in the case of the R = Me complex. The $\Delta H^{\#}$ (kcal/mole) and $\Delta S^{\#}$ (eu) values for the isomerisations *mer*-$Fe(MeQ)_3^- \rightarrow$ *fac*-$Fe(MeQ)_3^-$ and *fac*-$Fe(MeQ)_3 \rightarrow$ *mer*-$Fe(MeQ)_3$ are respectively 26·29, 11·27 and 23·20, 5·49. Unfortunately, activation parameters are often not good discriminators of possible alternative reaction pathways (Serpone and Bickley 1972). However the RQ^- ligand is rigid and planar and this may make the planar twist pathway favourable for the present species (Basolo *et al* 1953). It is certain that the isomerisation process is intramolecular as no mixed ligand complexes are formed when mixtures (e.g. R = Me and Cl) are allowed to coisomerise.

2.8 *Comments on isomer preference and future work*

The ferro- and ferriverdin family has provided model examples of the dependence of *tris* chelate geometry on metal oxidation state. In ferroverdins the low-spin bivalent metal displays a high degree of thermodynamic specificity for the *fac* geometry while in ferriverdin the low-spin trivalent metal shows a good degree of preference for *mer* geometry. Thus the metal oxidation state can recognise and differentiate the isomeric *fac* and *mer* N_3O_3 octahedra. Metastable populations of *mer*-ferroverdin and *fac*-ferriverdin can be generated but in each case the mismatch gets spontaneously corrected by isomerisation.

In general the *mer* configuration has a steric advantage over the *fac* geometry since the pendant oximato oxygen atoms have greater separation in the former (figure 2). If ligand distribution were statistical, $K^{III} = 3$. Observed K^{III} values are substantially larger (table 3) and this would be at least partly due to the above mentioned steric factor. However this factor can not explain the large stability of *fac*-$Fe(RQ)_3^-$ (very high K^{II}). The origin of this must be electronic and this is under further investigation. An extended Hückel molecular orbital study on $Mo(CO)_3(PH_3)_3^z$ has revealed that the stable $18e(z = 0, t_2^6)$ and $17e(z = 1, t_2^5)$ geometries are respectively *fac* and *mer* (Mingos 1979). We note that $Fe(RQ)_3^z(z = 0, -1)$ also form an $18e$–$17e$ pair.

The RQ complexes provide an unique opportunity for studying the pattern of *z*-geometry ($z = 0, -1$) relationship for the $3d$ transition metal ion complexes of type $M(RQ)_3^z$. Results in the case of nickel have been published (Ray and Chakravorty

Table 5. Equilibrium isomer population [R = Me in all cases except Cr(3,4-benzo); temperature is 298 K in all cases except $Mn(MeQ)_3^-$ (253 K); solvent is MeCN in all cases except M = $Mn(CH_2Cl_2)$ and M = $Co(CHCl_3)$].

%*mer*	$M^{II}(RQ)_3^-$		$M^{III}(RQ)_3$	%*mer*
—	Sc	d^1	Ti	—
—	Ti	d^2	V	—
—	V	d^3	Cr	46
—	Cr	d^4	Mn	100
81	Mn	d^5	Fe	85
0	Fe	d^6	Co	30
—	Co	d^7	Ni	98
44	Ni	d^8	Cu	—

1988). Here the bivalent metal is lax in its specificity in the *fac* form but the trivalent metal strongly favours *mer* geometry. This is quite different from the case of iron. Some results on equilibrium isomer populations for $Mn(RQ)_3^z$ and $Co(RQ)_3^z$ are also available (Basu and Chakravorty 1989, unpublished results) and a comparison is made in table 5. There are a number of gaps remaining to be filled in this table. Work is in progress to achieve this end and to rationalise the observed trends of isomer populations.

Acknowledgements

Financial assistance received from the Council of Scientific and Industrial Research, and the Department of Science and Technology, New Delhi, is gratefully acknowledged.

References

Basolo F, Hayes J C and Newmann H 1953 *J. Am. Chem. Soc.* **75** 5102
Basu P, Bhanja Choudhury S, Pal S and Chakravorty A 1989a *Inorg. Chem.* **28** 2680
Basu P, Pal S and Chakravorty A 1989b *J. Chem. Soc., Chem. Commun.* 977
Basu P, Pal S and Chakravorty A 1989c *J. Chem. Soc., Dalton Trans.* (in press)
Baudisch O 1940 *Science* **92** 336
Bleaney B and O'Brien M C M 1956 *Proc. Phys. Soc. London* **B69** 1216
Bond A M, Colton R and Kevekordes J E 1986 *Inorg. Chem.* **25** 749
Bursten B E 1982 *J. Am. Chem. Soc.* **104** 1299
Candeloro S, Grdenic' D, Taylor N, Thompson B, Viswamitra M and Hodgkin D C 1969 *Nature (London)* **224** 589
Chain E B, Tonolo A and Carilli A 1955 *Nature (London)* **176** 645
Charalambous J, Haines L I B, Morgan J S, Peat D S, Campbell M J M and Baily J 1987 *Polyhedron* **6** 1027
Cronheim G 1947 *J. Org. Chem.* **12** 1
Ehrenberg A 1956 *Nature (London)* **178** 379
Griffith J S 1961 *The theory of transition metal ions* (Cambridge: University Press) p. 364
Lahiri G K, Bhattacharya S, Ghosh B K and Chakravorty A 1987 *Inorg. Chem.* **26** 4324
Mingos D M P 1979 *J. Organomet. Chem.* **179** C29

Pal S, Melton T, Mukherjee R N, Chakravarty A R, Tomas M, Falvello L R and Chakravorty A 1985 *Inorg. Chem.* **24** 1250
Pal S, Mukherjee R N, Tomas M, Falvello L R and Chakravorty A 1986 *Inorg. Chem.* **25** 200
Pal S and Chakravorty A 1987 *Inorg. Chem.* **26** 4331
Ray D and Chakravorty A 1988 *Inorg. Chem.* **27** 3292
Serpone N and Bickley D G 1972 *Prog. Inorg. Chem.* **17** 391